Scientific Report to the NERC Geophysical Equipment Facility for SEIS-UK loan 885

Derek Keir[1], James Hammond[2]
[1]University of Southampton, [2]Imperial College London

Abstract
SEIS-UK provided a loan of 12 broadband seismic systems (12 x CMGESP), for deployment in a network of approximately 200km x 300km in the central and northern portions of the Afar depression. The network (loan 885) ran from October 2009 - October 2011, and was extended until January 2012 under an extension application. These systems recorded continuously at 50Hz with relatively minor data losses due to equipment problems. These data have been used to constrain locations, moment tensors and time series of seismicity during the May 2010 intrusion in the Dabbahu segment in Afar. The data show the intrusion was sourced from a segment centred reservoir and spread to both the north and south along the rift axis. Moment tensor inversion shows the earthquakes are normal dip slip faults. In addition, data has been used to understand pre-co, and post eruption deformation associated with the June 2011 eruption of Nabro volcano. Initial results demonstrate activity started around March 2011, and peaked during the 12 June 2011 during the eruption. Teleseismic data is being used to constrain lithosphere and asthenosphere structure beneath Afar, the Red Sea, Gulf of Aden and Yemen using surface-wave tomography. Results show segmented low velocity zones beneath the ocean ridges suggested segmented upwelling and partial melting of asthenosphere. In addition, teleseismic data is being used to constrain seismic structure of the transition zone beneath the region using body-wave teleseismic tomography and receiver function analysis. Results show Data was also incorporated into crustal receiver function, teleseismic body-wave tomography, Pn tomography, and SKS splitting analysis reported for SEIS-UK loan xxx.

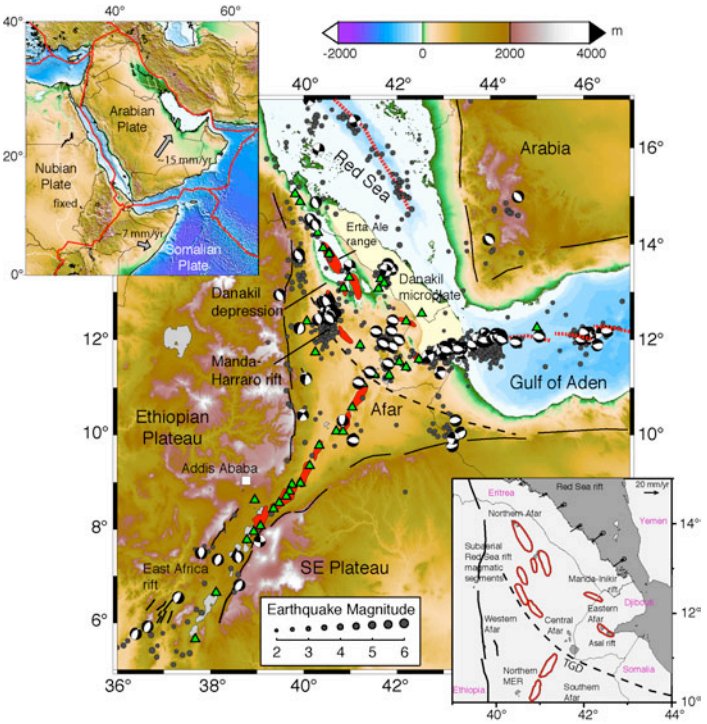

Figure 1. Tectonic setting of the Afar depression. Solid black lines show Oligocene-Miocene border faults of the Red Sea, Gulf of Aden Aden, and East African rifts. Red segments show the Quaternary-Recent subaerial rift axes, and green triangles show Holocene volcanoes. Dashed lines show the Tendaho-Goba'ad Discontinuity (TGD). The Danakil microplate is shaded yellow. Gray circles show large earthquakes during 1973–2012 sourced from the National Earthquake Information Center (NEIC) catalog. Earthquake focal mechanisms are from the Global Centroid Moment Tensor (CMT) catalog. **Top left inset**: topography of NE Africa and Arabia. Gray arrows show plate motions relative to a fixed Nubian plate (ArRajehi et al., 2010). Bottom right inset shows. **Botton right inset**: Zoom of Oligocene-Miocene border faults (black) and Quaternary-recent subaerial rift axes (red segments) showing motion of the Danakil microplate (McClusky et al., 2010).

Background
The Afar Depression (Figure 1) marks the intersection of the southern Red Sea rift (RSR), the Gulf of Aden rift (GOA) and the Main Ethiopian Rift (MER), forming an archetypal rift-rift-rift triple junction (e.g. McKenzie et al., 1972). The Afar rifts are the most mature part of the continental East-Africa Rift system and hosts the on-shore extension of the Red Sea and Gulf of Aden oceanic spreading (e.g. McKenzie et al., 1972). They are the only place on the planet where the transition from late-stage continental rifting to oceanic seafloor spreading is occurring subaerially today.

Recent active rifting and dike injection has focused scientific attention on this area (Ebinger et al., 2010). In September 2005, a 60km long segment of the Dabbahu-Manda-Hararo (DMH) rift segment opened in two weeks (Wright et al., 2006), and geodetic and seismic monitoring, using data mainly from this experiment, have revealed 14 episodes of dike injection along this segment of the rift (e.g. Wright et al., 2006, Ayele et al., 2009, Hamling et al., 2009, Belachew et al., 2011). Analysis of the most recent intrusion was one of the objectives of the study

described here.

Survey Procedure

The 12 ESPCMG seismometers from loan 885 were initially localized during October 2009-January 2011 around the Dabbahu segment of the Afar rift with the primary objective of investigating the on-going seismcity associated with dyking (Figure 2a). In February 2011, 7 of the seismometers were moved northward into the Danakil depression in order to record microseismicity in the northernmost basin of Afar (Figure 2b). During the project 2 ESPCMG sensors failed, and were replaced in October 2011 by 3 x 6TD sensors.

Help and collaboration from Addis Ababa University (in particular Dr Atalay Ayele), the National Regional Afar State government, the Federal Ethiopian Government and SEIS-UK employees was essential for the success of the project. Logistical procedures were already well-advanced following the 2005 NERC funded Urgency network and 2007-2009 Afar Consortium network in Afar. We located stations mainly in fenced compounds to maximize security. Care was taken to achieve a regular spacing of stations, but not at the expense of finding a secure location. Available locations were mainly limited to towns with a fenced government compounds (e.g., police stations, clinic, government offices). We could distribute the stations at regular intervals in the region, but were unable to access the eastern side of the Danakil depression due poor security conditions there. However our station distribution was adequate to achieve the scientific objectives (Figure 2).

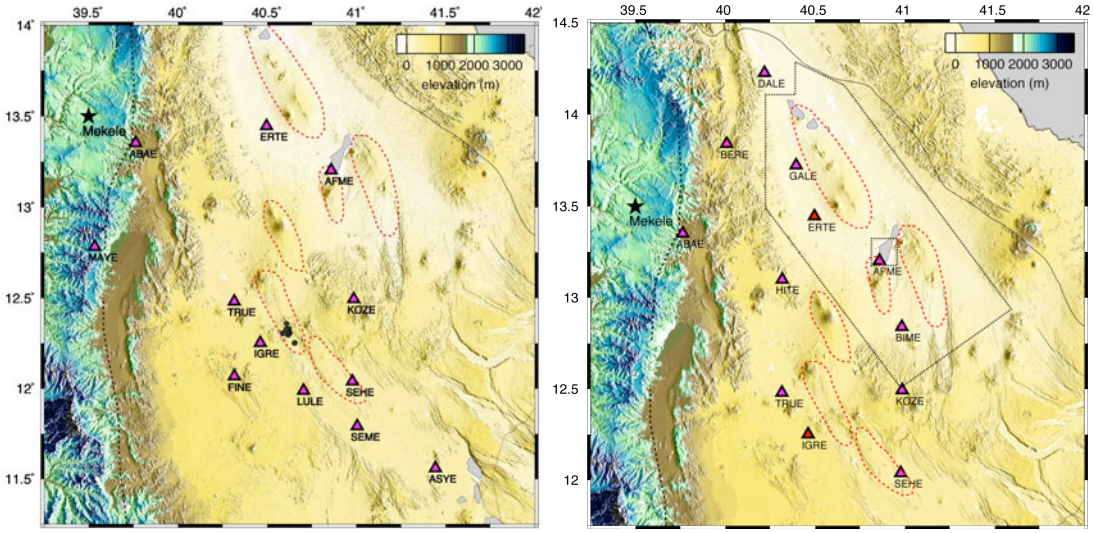

Figure 2. a - Left panel shows the distribution of seismic stations initially deployed in October 2009. b - The right panel shows the configuration of stations after moving a number of stations northward into the Danakil depression mainly during February 2011.

Most of the seismometers were deployed in a hole ~1-1.5m deep, ~0.7m in diameter. Seismometers were placed in a plastic bag and buried directly in the soil, with the sensor pits were protected from the heat using buried reflective sheets (Figure 3). A second hole close to the seismometer hole was dug, and a plastic bin placed inside. This was of a depth so that the bin was ~20cm above the surface. The battery, break out box, were placed in this box with all cables attached. Cables for the sensor and firewire led from this box to the seismometer hole. Cables for the GPS and solar panels led out of the box and connected with the solar panels and GPS antenna located nearby. All cables out of the box were fed through flexible plastic conduit and secured to posts or buried. The battery/cable box was then covered with insulation and plastic, and secured with tape. Before the box was secured the configuration of the sensors was checked using the palms for the ESP and 6TD. 3 seismic stations were deployed subaerially with the sensor deployed directly on bedrock and covered with a plastic bucket, then a cairn of fist sized rocks, and finally by several layers of reflective foil. For these subaerial deployments the battery and breakout box etc were placed in a bucket in a similar fashion for subsurface deployments except that the bucket was completely above the ground, and then protected by a cairn of stones and by reflective foil (Figure 3).

Figure 3. left panel shows a typical subsurface deployment and the right panel shows a typical subaerial deployments with both the sensor and battery/breakout box housing covered with a cairn of rocks and reflective foil.

Data Quality

The CMGESP systems were primarily used in the study and were generally user friendly. The data were generally of good to excellent quality and of relatively low noise, especially during the night. We encountered relatively few problems with the instruments. Instrumental problems were restricted to 3 of the ESP's being unable to lock during station removal. For these instruments, we removed 2 during the project and shipped back to SEIS-UK mid-project for replacement by the 3 x 6TDs. One instrument suffered from a failed horizontal component for the duration of the project. We had a few stations temporarily stop working due to battery failure, though this was relatively uncommon since we regularly replaced the batteries due the harsh temperature conditions. One solar panel was stolen during the project.

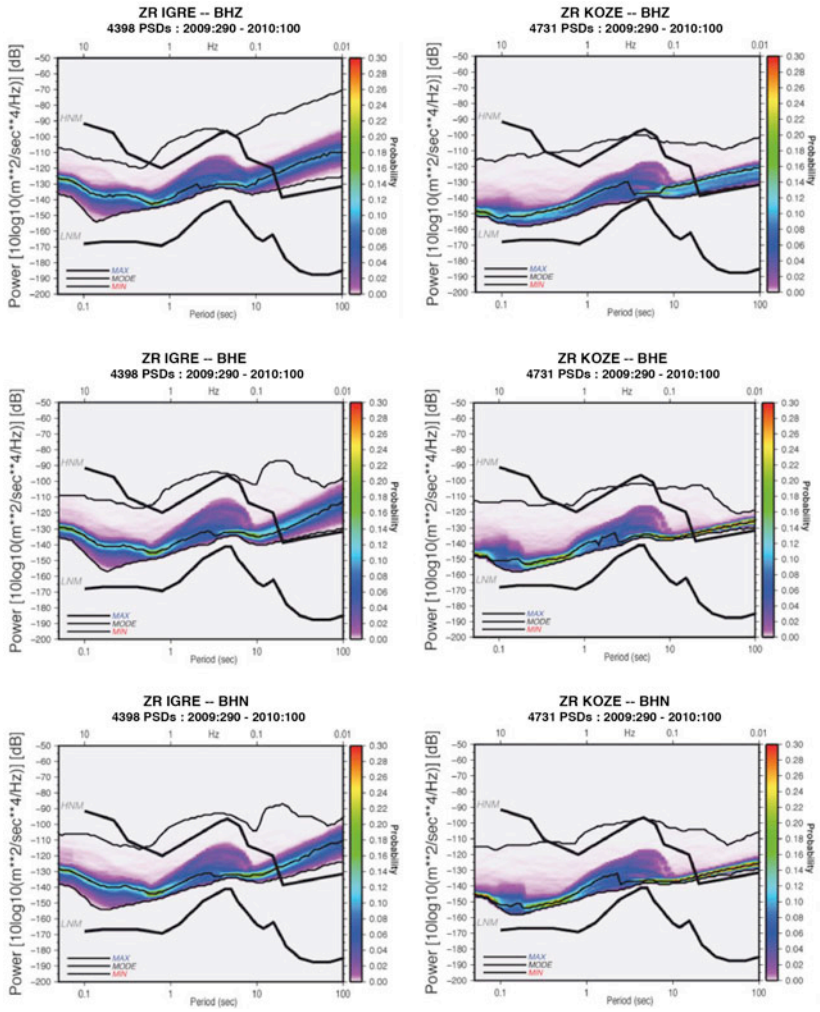

Figure 4. Power spectral density plots of the vertical components over a seismically quiet period. The stations show typical ambient noise at the stations across the network. The black lines show the high and low noise model of Peterson (1993). The modal value is shown as a coloured line.

Processing

Earthquake locations: Continuous seismic data for May 2010 and also for the whole of 2011 was initially loaded in 1-hour-long segments, and filtered using a bandpass filter of 1-10Hz. Data is manually inspected for earthquakes and arrival times of P-, and S-waves from earthquakes recorded at 3 or more seismic stations are measured. Provisional earthquake locations are computed using Hypo2000 for earthquakes including 4 or more P- or S-phases using a simple 4-layer, 1-D velocity model for the Afar crust, defined using wide-angle seismic reflection and refraction data (Makris and Ginzburg, 1987). We use a linear increase in seismic velocities within each crustal layer, a technique designed to avoid artificial clustering of earthquakes at sharp discontinuities in velocity associated with using a stepped mode. Our resultant locations have average horizontal errors of < 500 m and errors in depth of < 2km.

Earthquake magnitude, energy release and moment tensor inversion: Local magnitudes (M_L) of the earthquakes were computed from the maximum zero-to-peak amplitude measured on simulated horizontal component Wood-Anderson displacement seismograms after removal of instrument response [Richter, 1935]. These measurements are used in conjunction with hypocentral distances to estimate local magnitude (M_L) using the distance correction applicable to the MER (Keir et al., 2006). These analyses also show that the magnitude of earthquakes ranges M_L 0.4-4. Seismic moment release (Mo) is determined using the empirical relationship derived between M_L and Mo by Hanks and Kanamori (1979]. Earthquake moment tensors were computed from full waveform inversion using the code of Ford et al. (2009).

Teleseismic methods: Teleseismic surface-wave tomography was conducted using the 2-plane-wave technique of Yang and Forsyth (2008).

Interpretation and results

Seismicity

May 2010 intrusion - data collected during 17th - 31st May 2010 has been used to constrain locations and magnitudes of ~300 earthquakes occurring during the final dyke intrusion of the Dababhu rifting episode (Figure 5). The location, total opening, and total moment release of the intrusion is constrained using modeling of InSAR data (Figure 6). The seismicity constrains timing of intrusion and proportion of deformation by fault slip. The results show that seismicity initiates at around 8 km depth beneath the centre of the Dabbahu segment and migrates vertically upwards to around 3 km. Afterwards, seismicity migrates both northward and southward along the rift axis over a ~6-hour time period. The earthquakes are high frequency volcano-tectonic earthquakes with clear P-and S-phases and the migration of these earthquakes shows they are likely induced by a laterally propagating intrusion in the upper crust. The earthquakes induced by the faulting near the edge of the moving intrusion are normal dip slip earthquakes with T-axes parallel to the regional direction of extension.

Teleseismic imaging

Surface-wave tomography - dispersion curves of teleseismic earthquakes have been picked and inverted for phase velocity maps at periods ranging from 25 seconds to 125 seconds. The provisional results show that at 40 seconds the lowest S-wave velocities are beneath the central Ethiopian rift. Other distinct low velocity anomalies are beneath the Afar depression and also a segment of the central-west Gulf of Aden rift. The low velocity anomalies in the subaerial parts of the map are likely zones of magma intrusion in the mantle lithosphere, whereas the low velocity anomaly in the Gulf of Aden is likely upwelling asthenosphere beneath the axis of the ridge.

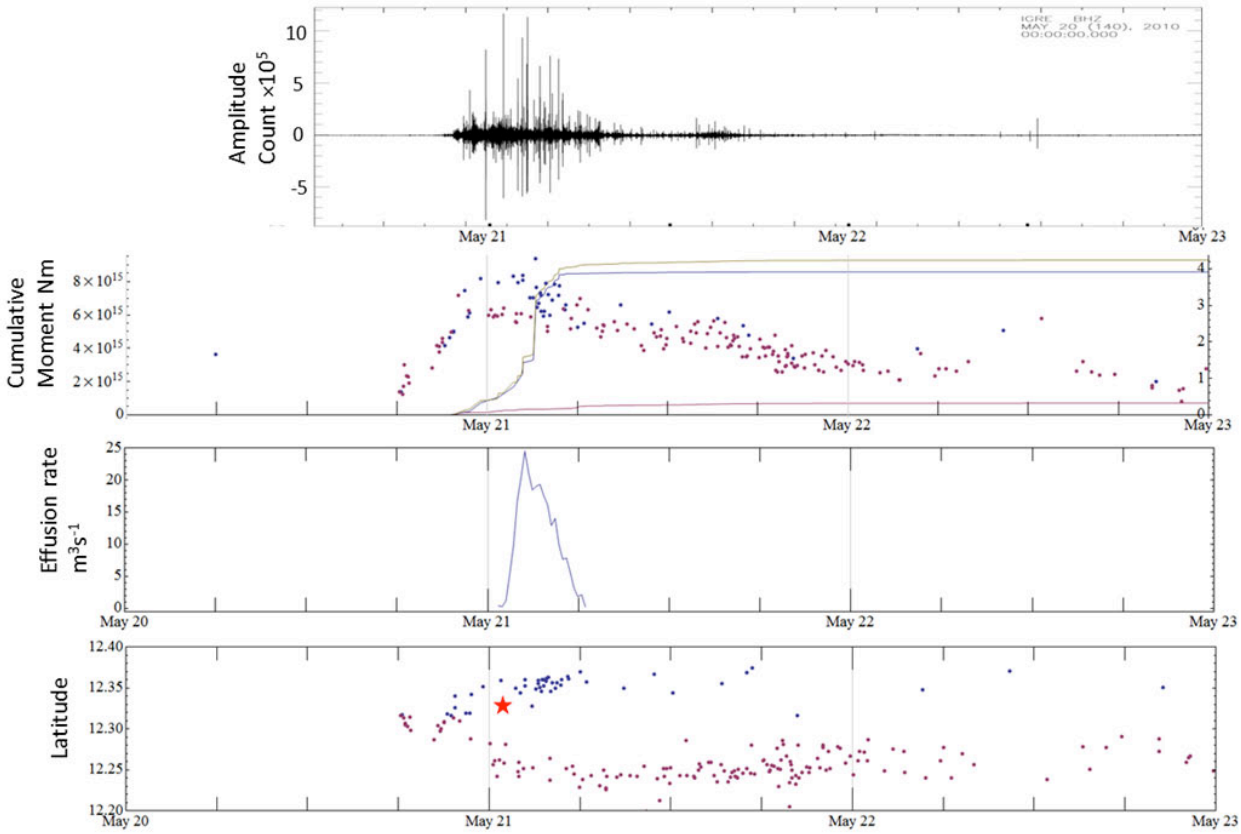

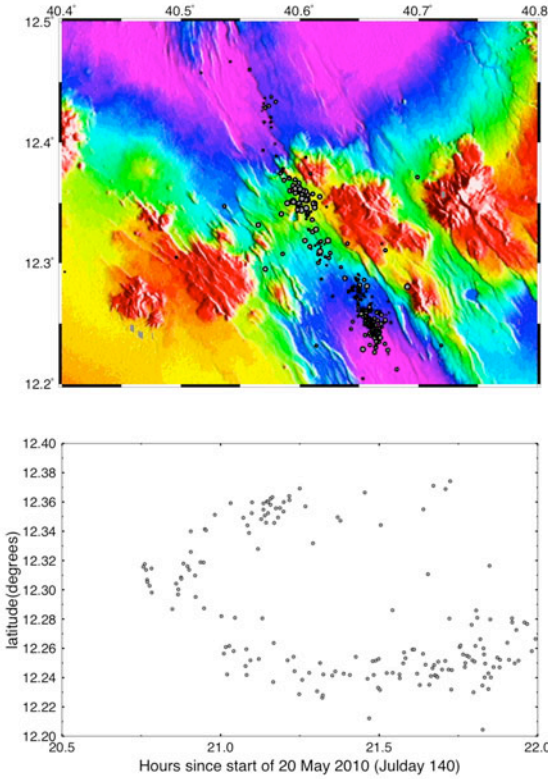

Figure 5. Left panel shows the location of the earthquakes induced by the May 2010 intrusion, and the lower plot shows the change in latitude of earthquakes through time. The diagram shows that earthquake activity started in the middle of the Dabbahu segment and migrated to the north and south during a ~6-hour-long time period.

Top panel is a figure illustrating the timing of seismic events and lava effusion. Top to bottom: (**a**) Vertical component seismic trace for station IGRE (**b**) Seismicity magnitudes and cumulative moment for all earthquakes within 3km of dyke model. Blue points show seismicity in northern dyke segment, red points show seismicity for southern dyke segment, blue curve shows cumulative seismic moment for northern dyke, red curve for southern dyke, yellow curve total cumulative seismic moment. (**c**) Effusion rate calculated from extracted SEVIRI band 3 (1.6 µm) radiance. (**d**) Migration of seismicity along dyke by latitude. Blue points are northern segment earthquakes, red point southern segment earthquakes, red star shows location and time of eruption onset. All earthquakes within 3km of the dyke are plotted.

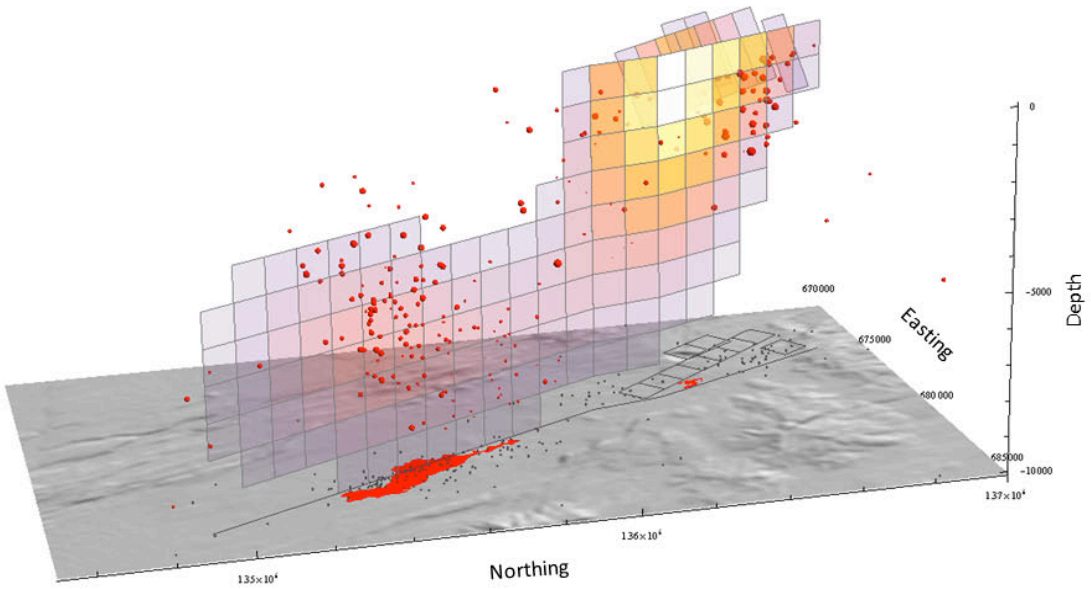

Figure 6. A perspective plot of modelled dike opening and seismicity. Dike opening shaded from purple (smallest opening) to white (largest), Earthquakes scaled by size. The projection of the deformation model grid onto the surface is shown in gray lines on hill shaded SRTM topography. The projection of earthquake locations is shown as gray dots, lava flows are shown as red polygons. The plot shows that earthquakes mainly occur around the edges of the dike and are therefore likely to be caused by localised extension stress near the dike tip induced by stress changes around the dike.

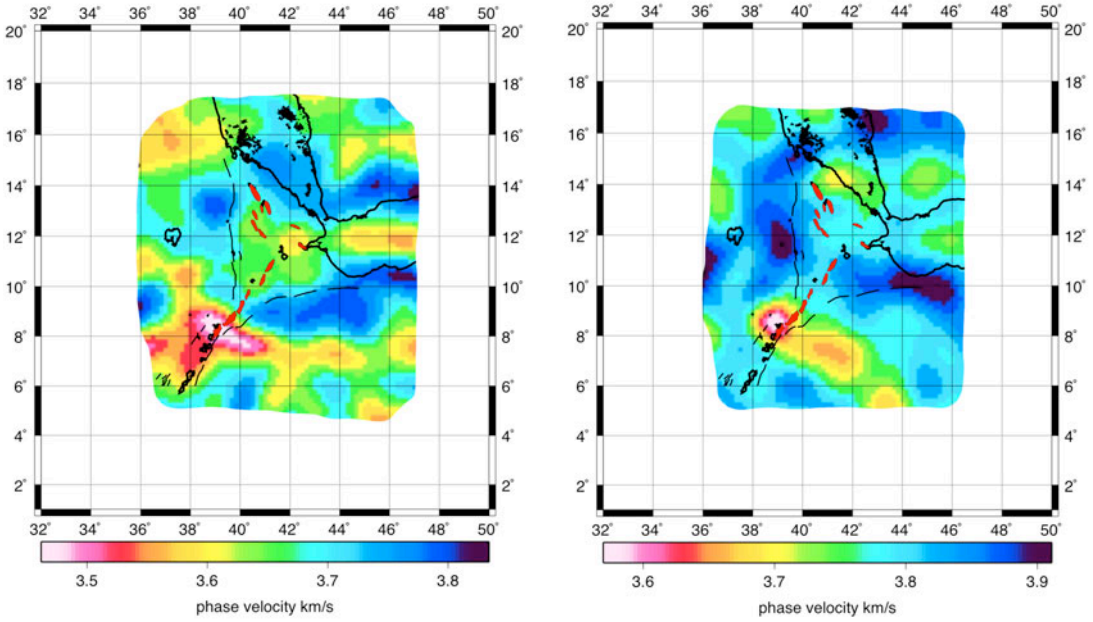

Figure 7. Phase velocity maps for periods 40 second (left) and 90 second (right) generated using inversion of teleseismic surface wave dispersion curves.

Conclusions and recommendations

These SEIS-UK loans have enabled collected of high quality data from one of the most inaccessible parts of the world. Up to 13 seismic stations were operated safely and continuously for just over 2 years. No seismometer was lost or stolen during the experiment and 2 seismometers were damaged because of instrument failure meaning they could not be locked. New analyses of seismicity, surface-and body-wave tomography, and receiver functions have been conducted on the data. Of these, the analysis of the May 2010 seismicity is near submission (Barnie et al., in prep), as is the receiver function study of the mantle transition zone beneath the region (Thompson et al., in prep). In addition, the data was used in already published analysis outlined in the Afar consortium loan report 841. These are namely the teleseismic body-wave study of the Ethiopian rift and Afar presented in Hammond at al.

(2013) in Geology, crustal receiver functions presented in Hammond et al. (2011), the Pn tomography study by Stork et al. (2013). These data have made a significant contribution to understand how magma intrudes the crust, the behaviour of border fault system, and also in constraining lithosphere scale deformation and melting processes during the breakup of continents.

Table of stations deployment details

Code	Inst.	Digitizer	Latitude	Longitude	Elev.	Deplyment date	Remover date	SR. Name
ASYE	3ESP	T34977	11.56070	41.44220	0370	2009:282:06:00:00	2011:051:00:00:00	50 Asaita
HITE	3ESP	T34977	13.10124	40.31691	0566	2011:053:07:00:00	2012:001:00:00:00	50 Haitan
ERTE	3ESP	T34591	13.44630	40.49690	-005	2009:292:06:00:00	2011:055:13:00:00	50 Erta_Ale
HALE	3ESP	T34591	13.84221	40.00772	0797	2011:058:05:00:00	2012:001:00:00:00	50 Berhale
BTIE	3ESP	T34573	11.19490	40.02180	1659	2009:284:07:00:00	2010:051:00:00:00	50 Bati
SAHE	3ESP	T34573	12.04015	40.97695	0365	2010:053:00:00:00	2012:031:04:30:00	50 Saha
MAYE	3ESP	T34589	12.78320	39.53430	2440	2009:280:11:00:00	2010:334:00:00:00	50 Maychew
DAME	3ESP	T34589	11.68684	40.96249	0424	2010:350:00:00:00	2011:045:00:00:00	50 Dam
GALE	3ESP	T34589	13.72514	40.39401	-087	2011:055:05:00:00	2012:001:00:00:00	50 Agale
AFME	3ESP	T34601	13.20396	40.85848	-058	2009:294:03:00:00	2012:001:00:00:00	50 Afdera
FINE	3ESP	T34739	12.06812	40.31597	0782	2009:283:12:00:00	2010:323:00:00:00	50 Finto
LAVE	3ESP	T34739	13.60449	40.65789	0599	2010:326:00:00:00	2011:055:00:00:00	50 Lava
ERTE	3ESP	T34739	13.44630	40.49690	-005	2011:055:13:00:00	2011:284:00:00:00	50 Erta_Ale
TRUE	3ESP	T34599	12.48125	40.31481	0381	2009:284:05:00:00	2011:253:00:00:00	50 Teru
AHME	3ESP	T34599	14.08887	40.27840	0046	2011:259:00:00:00	2012:001:00:00:00	50 Ahamed_Ella
IGRE	3ESP	T34398	12.25259	40.46123	0675	2009:284:00:00:00	2012:001:00:00:00	50 Igra_Lita
LULE	3ESP	T34732	11.98922	40.70370	0594	2009:289:10:00:00	2011:051:00:00:00	50 Alelu
BIME	3ESP	T34732	12.84183	40.98386	0054	2011:052:08:00:00	2011:284:00:00:00	50 Bidou
KOZE	3ESP	T34731	12.49478	40.98489	0543	2009:288:07:00:00	2012:001:00:00:00	50 Kori
ABAE	3ESP	T34510	13.35350	39.76355	1447	2009:292:00:00:00	2012:001:00:00:00	50 Abala
SEME	3ESP	T34636	11.79258	41.00433	0433	2009:287:07:00:00	2011:049:15:00:00	50 Semera
DALE	3ESP	T34636	14.22897	40.21783	-097	2011:056:12:00:00	2012:001:00:00:00	50 Dallol
ERTE	6T	T6108	13.44630	40.49690	-005	2011:297:00:00:00	2012:001:00:00:00	50 Erta_Ale
GULE	6T	T6083	13.69449	39.58854	2021	2011:330:00:00:00	2012:001:00:00:00	50 Agula
GPSE	6T	T6093	13.48817	40.52833	0000	2011:275:00:00:00	2012:001:00:00:00	50 GPS_station

References

Ayele, A., D. Keir, C. Ebinger, T.J. Wright, G.W. Stuart, W.R. Buck, E. Jacques, G. Ogubazghi, J. Sholan (2009), September 2005 mega-dike emplacement in the Manda-Harraro nascent oceanic rift (Afar Depression), Geophys. Res. Lett., 36, L20306.

Barnie, T., M. Belachew, I. Hamling, B. Hoffman, D. Keir, D. Eastwell, J. Hammond, C. Oppenheimer, T. Wright, A. Ayele, (in prep), The May 2010 intrusion and eruption of the Manda Harraro rift, Geol. Soc. Lond. Spec. Pub.

Bastow, I.D., D. Keir (2011), Protracted development of a magmatic rifted margin in Afar, Nature Geoscience, 4, doi: 248-250.

Belachew, M., C. Ebinger, D. Cote, D. Keir, J. Rowland, J.O.S. Hammond, A. Ayele (2011), Comparison of dike intrusions in an incipient seafloor spreading segment in Afar, Ethiopia: Seismicity perspectives, J. Geophys. Res. 116, B06405.

Ebinger, C., A. Ayele, D. Keir, J. Rowland, G. Yirgu, T. Wright, M. Belachew, I. Hamling (2010), Length and timescales of rift faulting and magma intrusion: the Afar rifting cycle from 2005 to present, Annu. Rev. Earth Planet. Sci., 38, 437-464.

Ford, S.R., D.S. Dreger, W.R. Walter (2009), Source analysis of the Memorial Day explosion, Kimchaek, North Korea, Geophys. Res. Lett., 36, L21304.

Hammond, J.O.S., J-M. Kendall, G.W. Stuart, C.J. Ebinger, I.D. Bastow, D. Keir, A. Ayele, M. Belachew, B. Goitom, G. Ogubazghi, T.J. Wright, (2013), Mantle upwellings and initiation of rift segmentation beneath the Afar Depression, Geology 41, 635-638.

Hammond, J.O.S., J-M. Kendall, G. Stuart, D. Keir, C. Ebinger, A. Ayele, M. Belachew (2011), The nature of the crust beneath the afar triple junction: Evidence from receiver functions, Geochem. Geophys. Geosyst., 12, Q12004.

Hanks, T. C., and H. Kanamori (1979), A moment magnitude scale, J. Geophys. Res., 84, 2348–2350.

Keir, D., G. W. Stuart, A. Jackson, and A. Ayele (2006), Local earthquake magnitude scale and seismicity rate for the Ethiopian rift, Bull. Seismol. Soc. Am., 96, 2221 2230, doi:10.1785/0120060051.

Makris, J., and A. Ginzburg (1987), The Afar Depression: Transition between continental rifting and sea-floor spreading, Tectonophysics, 141, 199–214.

McKenzie, D.P., D. Davies, and P. Molnar (1972), Plate tectonics of the Red Sea and East Africa, Nature, 224, 125-133.

Peterson, J. (1993), Observations and modelling of seismic background noise, U.S. Geol. Surv. Open File Rep., 93-322, 1-95.

Richter, C. F. (1935), An instrumental earthquake magnitude scale, Bull. Seismol. Soc. Am., 25, 1–32.

Stork, A.L., G.W. Stuart, C.M. Henderson, D. Keir, J.O.S. Hammond (2013), Uppermost mantle (Pn) velocity model for the Afar region, Ethiopia: An insight into rifting processes, Geophys. J. Int. 193, 321-328.

Wright, T., C. J. Ebinger, J. Biggs, A. Ayele, G. Yirgu, D. Keir and A. Stork (2006), Magma-maintained rift segmentation at continental rupture in the 2005 Afar dyking episode, Nature, 442, 291-294.

Yang, Y. and D.W. Forsyth (2008), Attenuation in the upper mantle beneath Southern California: physical state of the lithosphere and asthenosphere, J. Geophys. Res., 113, B03308.